

Carbon production by thermal methane cracking in tubular quartz reactor

E. Busillo*, **A. Nobili****, **F. Serse****, **M.P. Bracciale***, **P. De Filippis***, **M. Pelucchi****, **B. de Caprariis***

emmanuel.busillo@uniroma1.it

* Department of Chemical Engineering, Materials and Environment, Sapienza University of Rome, Via Eudossiana 18, 00184, Roma, Italy

** CRECK Modeling Lab, Department of Chemistry, Materials and Chemical Engineering “Giulio Natta”, Politecnico di Milano, Piazza Leonardo da Vinci 32, 20133, Milano, Italy

Abstract

Methane cracking is explored as a bridge technology that enables the production of hydrogen while capturing carbon in the form of valuable materials, which could potentially lower hydrogen production costs and reduce carbon emissions. The process of methane (CH₄) cracking consists in the conversion CO₂-free of methane molecules into carbon and hydrogen



The valorization of the carbon product plays a crucial role in reducing H₂ prices and improving overall process economics. To achieve this, a comprehensive understanding of the complex network of reactions involved in methane thermal cracking is essential, particularly in relation to the formation of valuable carbon and unwanted byproducts such as carbon nanoparticles. The study focuses on the experimental analysis and kinetic modelling of methane cracking in a tubular quartz reactor, exploring the morphology of the carbon products. The experimental investigation of pure methane cracking in a tubular quartz reactor, was conducted operating within a temperature range of 875–975 °C and varying initial flow rates of CH₄ (30, 45, and 60 ml/min). The data obtained from experiments were compared to the outcomes of kinetic simulations conducted on a heterogeneous plug flow reactor with specific dimensions (length = 20 cm, diameter = 1.5 cm) using the OpenSMOKE++ framework [1]. The reactor model, which includes details of the sectional area, total inlet and outlet flow, and stream composition in mass fractions, has been previously explained in [2]. Surface deposition properties are defined by the superficial site fraction density ($\Gamma = 8 \times 10^{14} \text{ \#}/\text{cm}^2$) and surface composition expressed as surface fraction adopting a 50/50 ratio of armchair to zigzag edges, which is based on estimates from prior research studies [3,4]. The detailed chemical kinetic mechanism utilized in this study comprises three main components:

- 1) gas-phase mechanism incorporating detailed high-temperature kinetics from

- hydrogen and methane to polycyclic aromatic hydrocarbons (PAHs) formation;
- 2) carbon nanoparticle formation mechanism, validated against soot measurements in flames and flow reactors, utilizing a discrete sectional approach to describe large gas-phase aromatic species, soot particles, and aggregates;
 - 3) solid carbon deposition mechanism based on previous research [2], involving a variety of surface species and reactions to describe the reactivity of armchair and zigzag sites on a graphite substrate;

These mechanisms collectively comprise a total of 244 species and 9493 reactions, encompassing various physical and chemical processes such as inception, growth, dehydrogenation, particle coalescence, and aggregation to model the evolution of soot. Results of quantitative measurements of CH₄ conversion obtained from mass spectrometry data and the identification of key aromatic precursors acquired by GC/MS are depicted in the figures (Fig. 1, 2). The empirical findings and simulated outcomes align closely within the margins of experimental uncertainties. Methane conversion diminishes under two conditions: firstly, as the initial flow rate rises while temperature remains constant, due to a reduction in the mean residence time; and secondly, as temperature decreases while the initial flow rate remains fixed. When the flow rate is constant, a temperature shift from 875 to 975 °C corresponds to a methane conversion increase of approximately 28–30%. The maximum conversion rate is achieved at the highest temperature and residence time, with methane conversion reaching around 35% at T = 975 °C.

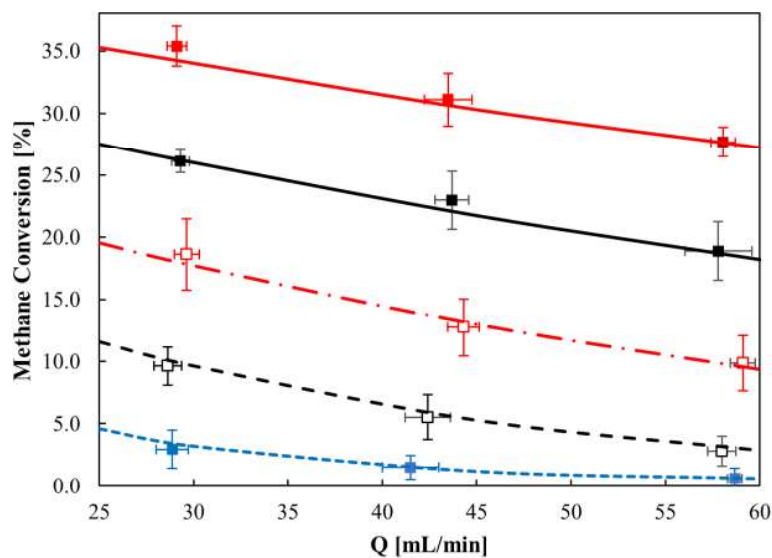


Figure 1. Methane conversion as a function of initial flow rates (25 – 60 ml/min) at different temperatures: 875 (blue), 900 (dashed black), 925 (dash-dotted red), 950 (black) and 975 °C (red). Symbols – experimental data; lines – model results.

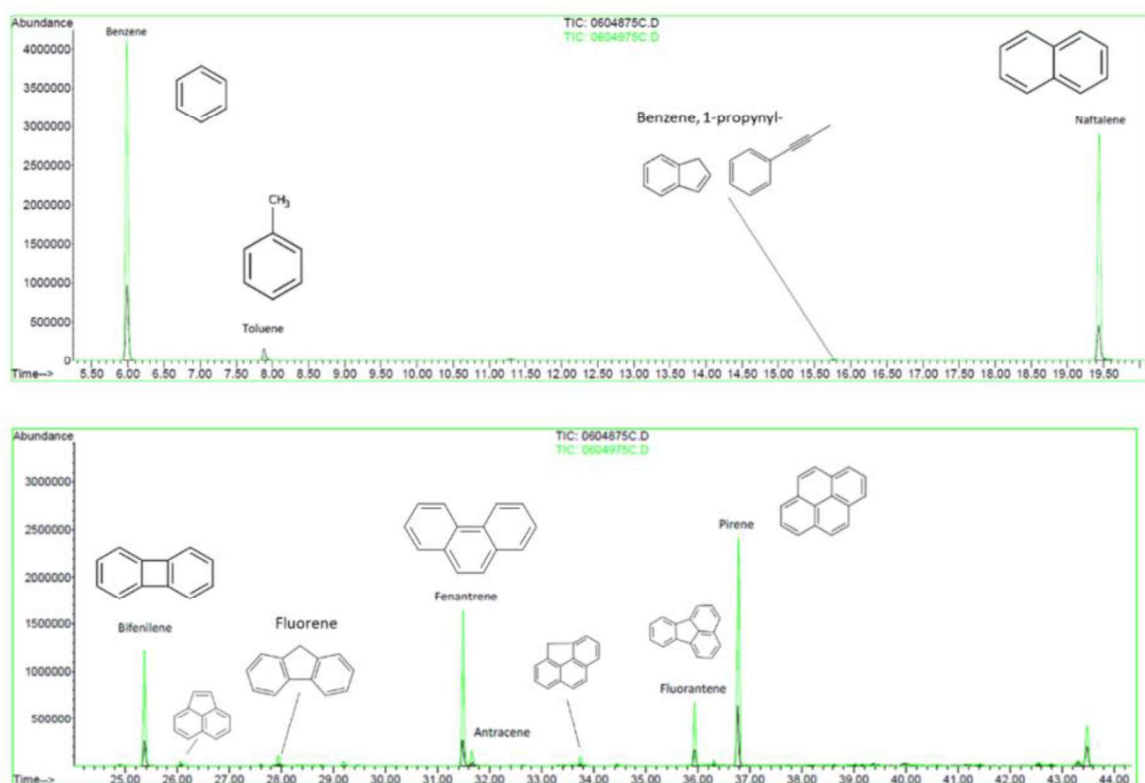


Figure 2. Chromatograms obtained from the injection into the GC/MS of gas samples taken from the top of the reactor.

The analysis of reaction intermediates revealed benzene, toluene, and PAHs such as naphthalene, phenanthrene/anthracene and pyrene. Benzene derivatives, biphenylene and fluoranthene have also been detected. Detailed analysis and characterization of the carbon products allowed for the exploration of the different morphologies for deposited carbon at reactor walls (Fig. 3 a, c) and carbon nanoparticles found in the gas phase (Fig. 3 b, d). The latter consist in fractal-like particles with dimensions of approximately 200–300 nm. On the other hand, deposited carbon is characterized by a carbonaceous matrix with interconnected hemispheres reaching sizes of up to 10 μm . Stacked dense carbon layers contribute to a thickness of 9–10 μm . The observed microstructures could be influenced by the chemical species deposited and their sticking characteristics. The mode of deposition (autocatalytic sticking mode of C_2 versus random deposition mode of C_6) affects the growth dimensionality. The transition between different microtextured pyrocarbons is expected to be linked to a threshold concentration of heavy polyaromatic molecules, which influence surface coverage and growth orientation. Vertical expansion of islands is attributed to lower adhesion energy on the substrate compared to cohesive energy within the pyrocarbon. As a result, proper control of gas-phase reactions is essential for regulating island growth and achieving the desired form of carbon.

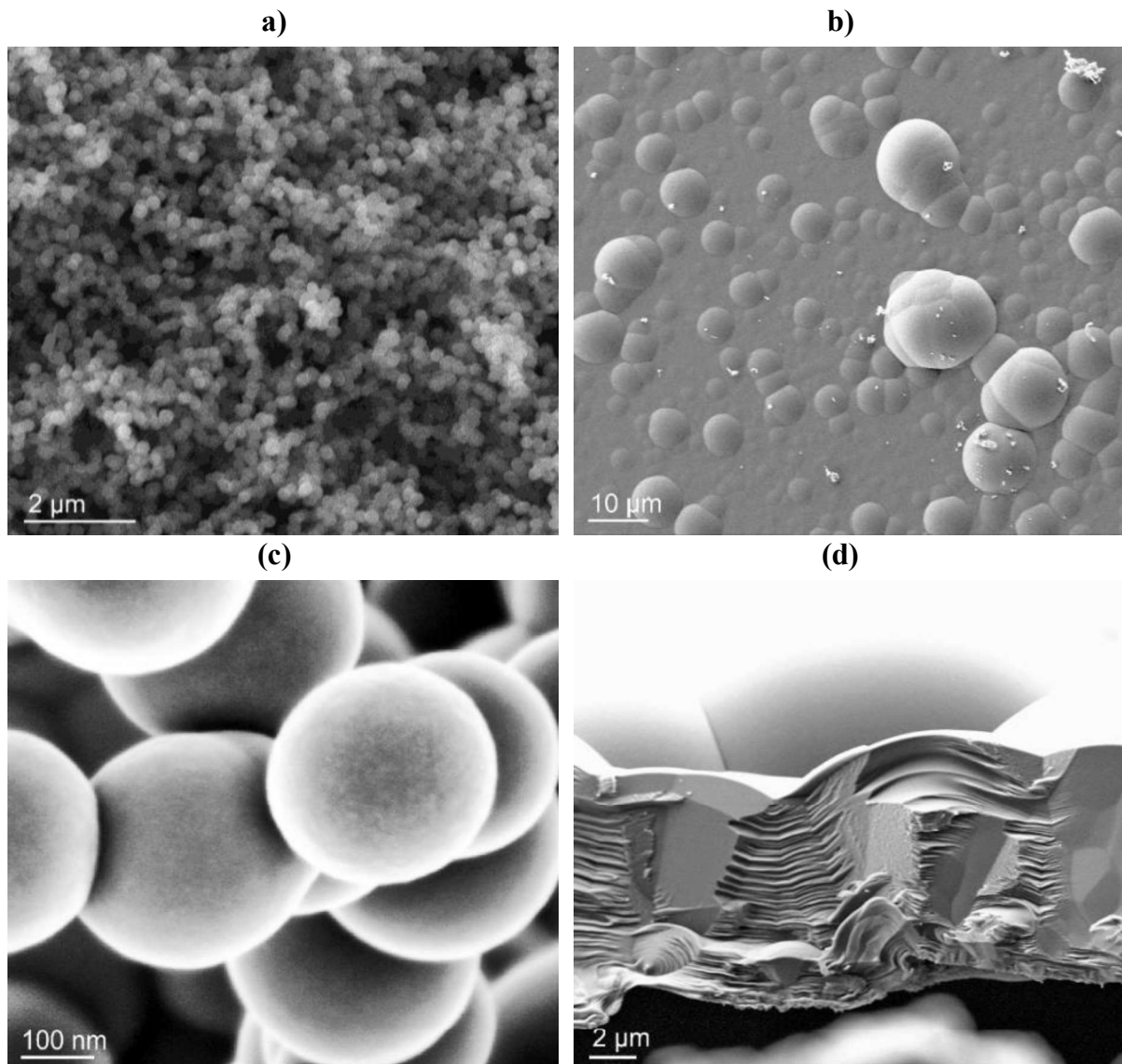


Figure 3. SEM images of the carbons collected: **a)** from the gas phase; **b)** from the reactor wall at $T = 925\text{ }^{\circ}\text{C}$, $Q_0 = 30\text{ mL/min}$ and $t = 1.5\text{ h}$. **c)** and **d)** micrographs represent the magnification of particles collected from the gas flow and the cross section of the flake collected from the reactor wall, respectively.

At the experimental condition of this work micro filamentous carbon structures with semispherical tip and homogeneous diameter resembling catalyst-free vapor grown carbon fibers [5] and carbon micro-trees already reported in catalyst-free propylene [6] and in methane deposition [7] have been observed. An example for such structures is represented in Fig. 4, a. The scheme of the proposed mechanism for the formation of these peculiar carbon arrangements is depicted in Fig. 4, b. Filaments could have been formed from early carbon structures grown in the gas-phase owed to high residence time of the gas inside the heated zone and to the low S/V ratio of the experimental reactor, thus suggesting a complex interaction between

homogeneous processes and deposited carbon morphology.

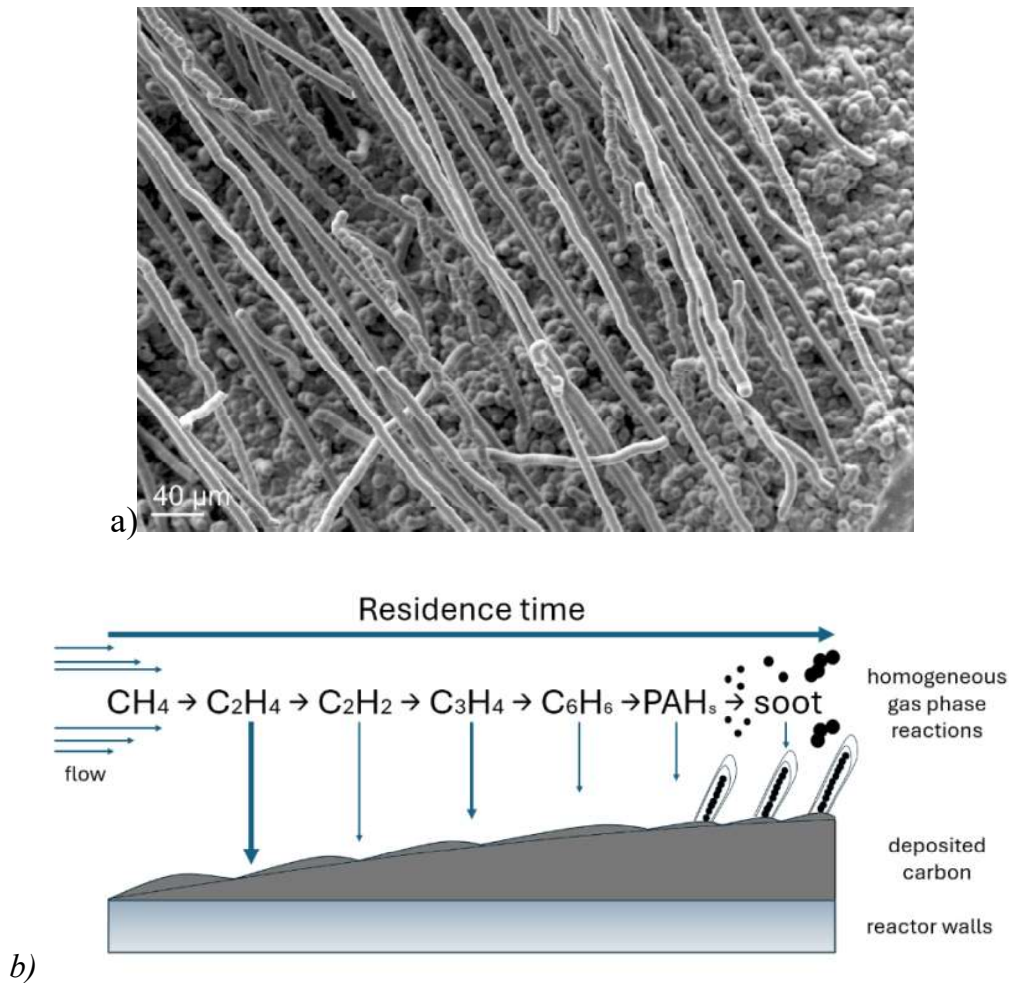


Figure 4. SEM Image of carbonaceous filaments produced at 925 °C after 3 h of reactor operation (a) and a scheme of the proposed mechanism for such filament formation (b)

In conclusion, this study delves into the experimental investigation of methane pyrolysis for carbon and hydrogen production, conducted within a tubular quartz flow reactor. By varying temperature and flow rates, the research elucidates the significant impact of these parameters on methane conversion rates. Through quantitative measurements and identification of key intermediates, such as aromatic and polyaromatic species, the study leveraged an existing kinetic model to interpret the observed results effectively. Moreover, the analysis of collected carbonaceous materials revealed distinct morphologies indicative of different formation mechanisms, heavily influenced by operating conditions and gas-phase composition. This nuanced understanding suggests a complex interplay between homogeneous and heterogeneous processes, further emphasized by the presence of carbon filaments with varying characteristics. Looking ahead, the study advocates for the extension of the kinetic model to encompass detailed pathways of aromatic species, polyaromatic hydrocarbons, carbon nanoparticles and surface deposition. Such

enhancements, coupled with systematic experimental characterization, hold the promise of providing stakeholders with advanced chemical kinetics and reactor modeling tools. These tools, in turn, are vital for driving the design of innovative technologies geared towards efficient hydrogen and valuable carbon materials production via hydrocarbon pyrolysis. Thus, this research paves the way for future advancements in the field, bridging the gap between fundamental understanding and practical applications.

References

- [1] Cuoci, A., Frassoldati, A., Faravelli, T., Ranzi, E., “OpenSMOKE++: an object-oriented framework for the numerical modeling of reactive systems with detailed kinetic mechanisms”, *Comput. Phys. Commun.* 192: 237–264 (2015)
- [2] Serse, F., Ding, Z., M. Bracconi, M., Maestri, M., Nobili, A., Giudici, C., Frassoldati, A., Faravelli, T., Cuoci, A., Pelucchi, M., “A comprehensive kinetic framework for solid carbon deposition and hydrogen production from the pyrolysis of light hydrocarbons streams”, *Carbon Trends*. 11: 100263 (2023)
- [3] Frenklach, M., Wang, h., “Detailed surface and gas-phase chemical kinetics of diamond deposition”, *Phys. Rev. B*. 43: 1520–1545 (1991)
- [4] Lacroix, R., Fournet, R., Ziegler-Devin, I.P., Marquaire, P.M., “Kinetic modeling of surface reactions involved in CVI of pyrocarbon obtained by propane pyrolysis”, *Carbon*. 48:132–144 (2010)
- [5] Zou, J.Z., Zeng, X.R., Xiong, X.B., Tang, H.L., Li, L., Liu, Q., Li, Z.Q., “Preparation of vapor grown carbon fibers by microwave pyrolysis chemical vapor deposition”, *Carbon*. 45: 828–832 (2007)
- [6] Fan, Z., Tan R., He, K., Zhang, M., Peng, W., Huang, Q., “Low temperature growth of catalyst-free carbon micro-trees”, *J. Mater. Sci.* 50:13–20 (2015)
- [7] Ajayan, P.M., Nugent, J.M., Siegel, R.W., Wei, B., Kohler-Redlich, P., “Growth of carbon micro-trees”, *Nature*. 404:243–243 (2000)